

# THEORETICAL ANALYSIS ON THE GEOEFFECTIVENESS OF A SHOCK OVERTAKING A PRECEDING MAGNETIC CLOUD

Y. M. WANG, P. Z. YE, S. WANG and M. XIONG

*School of Earth and Space Sciences, University of Science and Technology of China, Hefei, China  
(e-mail: wym@mail.ustc.edu.cn)*

(Received 17 May 2003; accepted 17 June 2003)

**Abstract.** The shock compression of the preexisting southward directed magnetic field can enhance a geomagnetic disturbance. A simple theoretical model is proposed to study the geoeffectiveness of a shock overtaking a preceding magnetic cloud. Our aim is to answer theoretically the question how deep the shock enters into the cloud when the event just reaches the maximum geoeffectiveness. The results suggest that the minimum value of  $Dst^*$  decreases initially, then increases again while the shock propagates from the border to the center of the cloud. There is a position where the shock compression of the preceding cloud obtains the maximum geoeffectiveness. In different situations, the position is different. The higher the overtaking shock speed is, the deeper is this position, and the smaller is the corresponding  $Dst_{\min}^*$ . Some shortcomings of this theoretical model are also discussed.

## 1. Introduction

Magnetic clouds (MCs) are subsets of coronal mass ejections (CMEs) (Wilson and Hildner, 1984). Nearly half of all CMEs form MCs in interplanetary space (Klein and Burlaga 1982; Gosling *et al.*, 1992; Cane, Richardson, and Wibberenz, 1997). MCs can be clearly identified by their characteristics including enhanced magnetic field strength, large and smooth rotation of magnetic field vector and low proton temperature (Burlaga *et al.*, 1981). Due to the MCs' relatively regular magnetic field, large intervals of southward component  $B_s$  of magnetic field usually can be formed within them, which has been widely considered the major interplanetary cause of moderate to intense geomagnetic storms, especially during the solar maximum (Sheeley *et al.*, 1985; Tsurutani *et al.*, 1988; Gosling *et al.*, 1991; Gonzalez, Tsurutani, and Gonzalez, 1999). Geomagnetic storms which are primarily defined by the enhanced ring current at the Earth's equator, can be indicated by the  $Dst$  index.

However, for highly intense geomagnetic storms, the interplanetary origin is not merely the MCs. A complex structure containing MCs is often of much more geoeffectiveness (e.g., Burlaga, Plunkett, and St. Cyr, 2002). Wang *et al.* (2003) presented the events of a shock overtaking a preceding MC which were all responsible for large geomagnetic storms. Especially, the 6 November 2001 event produced a great geomagnetic storm with  $Dst$  peak value of  $-292$  nT. Wang, Ye, and Wang (2003a) also analyzed the interplanetary origin of the largest geomag-



netic storm ( $Dst_{\min} = -387$  nT) during 2000–2001. The result suggests that a special complex structure, namely a multiple magnetic cloud (Wang, Wang, and Ye, 2002), created this great geomagnetic storm. During the solar maximum, the rate of CMEs occurrence is about 3–4 per day (Webb and Howard, 1994). Thus, it is worth studying such a complex structure because of its possible extraordinary geoeffectiveness.

Here, we try to theoretically study the geoeffectiveness of a shock overtaking a preceding MC. It is not a new idea that the shock compression of the preexisting southward component of magnetic field can increase geoeffectiveness of the corresponding  $B_s$  event. Tsurutani *et al.* (1992a) found that 3 of 5 great geomagnetic storms were caused by shock compression of preexisting southward interplanetary magnetic field. However, the events of a shock overtaking a MC associated with very large geomagnetic storms seem not to be presented until recently (Wang *et al.*, 2003). Although some authors have reported similar events (Burlaga, Behannon, and Klein, 1987; Lepping *et al.*, 1997), the contribution of a shock compressing preceding MCs in producing intense geomagnetic storms was small in those events because the compressed preexisting magnetic fields were northward.

On the basis of these events, we ask the following two questions naturally: What is the condition such that the overtaking shock is able to increase the MCs geoeffectiveness? How deeply does the shock enter the preceding MC when the geoeffectiveness of the event reaches maximum? As for the first question, the answer seems to be apparent. The necessary condition is that the magnetic field ahead of the shock should have southward component. As for the second question, the answer is complicated. The overtaking shock should lose energy while advancing into the preceding MC, and the compression ratio at the shock lies at the local Alfvénic Mach number. Thus, the corresponding geoeffectiveness of such an event will change for the different penetration depths of the shock relative to the cloud.

In the next section, the theoretical model is presented in detail. According to this model, we give the results, which show the change of the geoeffectiveness while the shock keeps advancing into the cloud, in Section 3. Finally, we discuss some shortcomings of this model and summarize the paper in Section 4.

## 2. Theory

### 2.1. MAGNETIC CLOUD

A typical magnetic cloud can be modeled by a local force-free flux rope (Burlaga 1988; Kumar and Rust, 1996). In cylindrical coordinates  $(R, \Phi, Z)$ , a force-free field with constant  $\alpha$  is given by the Lundquist solution (Lundquist, 1950)

$$B_R = 0, \quad B_\Phi = H B_0 J_1(\alpha R), \quad B_Z = B_0 J_0(\alpha R), \quad (1)$$

where  $B_0$  is the magnetic field amplitude at the cloud's axis,  $H = \pm 1$  indicates the handedness of the magnetic field, and  $J_0, J_1$  are the Bessel function of order 0 and

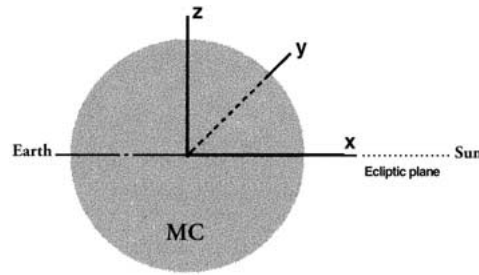


Figure 1. Sketch of the magnetic cloud's configuration.

1, respectively. The boundary of the flux rope is reached at the position of the first zero of  $J_0$ , i.e.,

$$J_0(\alpha R_0) = 0, \quad (2)$$

where  $R_0 = 2.41/\alpha$  is the radius of the flux rope.

By using this model, Lepping *et al.* (1997) fitted many observed magnetic clouds. They concluded that the clouds' axes are  $-15^\circ \pm 47^\circ$  in the  $\theta$  direction and  $102^\circ \pm 34^\circ$  in  $\phi$ , respectively. The  $\theta$  indicates the elevation of the axis aspect to the ecliptic plane and the  $\phi$  indicates the angle between the axis and the Sun–Earth line in the ecliptic plane. Therefore, in our theoretical analysis, we assume that the magnetic cloud is moving along the Sun–Earth line, and its axis is in the ecliptic plane and perpendicular to the Sun–Earth line, as shown in Figure 1. By this assumption, a hypothetical spacecraft detects the cloud along the  $x$ -axis and passes through its center, so the observed magnetic field only has  $y$  and  $z$  components, which are given by

$$B_y = -B_z, \quad (3)$$

$$B_z = B_\phi. \quad (4)$$

$B_z$  reaches the extreme value at the position  $J_1(\alpha d) = \alpha d J_0(\alpha d)$ , i.e.,  $d = 0.76 R_0$ , where  $d$  is the distance from the cloud's center.

## 2.2. OVERTAKING SHOCK

We introduce a fast forward shock behind the magnetic cloud. The shock may be produced by some fast moving ejecta. The size of the compressed region between the shock and its driver gas is usually comparable to that of the cloud (Zhang and Burlaga, 1988; Erkaev *et al.*, 1995). We assume that the overtaking shock is also moving toward the Earth and its nose is on the  $x$ -axis. Hence, the complicated situation is reduced to a relatively simple situation of an exactly perpendicular shock due to the absence of  $x$  component of the magnetic field within the cloud on the Sun–Earth line.

In ideal MHD, we can relate the plasma states upstream (denoted by subscript ‘u’) and downstream (denoted by subscript ‘d’) of the shock by using Rankine–Hugoniot relations:

$$[\rho u_n] = 0, \quad (5)$$

$$\left[ \rho u_n \mathbf{u}_t - \frac{B_n}{\mu_0} \mathbf{B}_t \right] = 0, \quad (6)$$

$$\left[ \rho u_n^2 + p + \frac{B^2}{2\mu_0} \right] = 0, \quad (7)$$

$$\left[ \rho u_n \left( \frac{1}{2} u^2 + \frac{\gamma}{\gamma - 1} \frac{p}{\rho} \right) + u_n \frac{B^2}{\mu_0} - \frac{B_n}{\mu_0} \mathbf{u} \cdot \mathbf{B} \right] = 0, \quad (8)$$

$$[B_n] = 0, \quad (9)$$

$$[u_n \mathbf{B}_t - B_n \mathbf{u}_t] = 0. \quad (10)$$

Here  $\mathbf{u}$  is the velocity of the plasma in the reference frame of the shock,  $\mathbf{B}$  is the magnetic field,  $\rho$  is the mass density,  $p$  is the gas pressure,  $\gamma$  is the polytropic index, and subscripts n and t indicate the components perpendicular and tangential to the discontinuity, respectively. The symbol  $[F] \equiv F_u - F_d$  denotes the difference of the quantity  $F$  across the discontinuity surface.

In the case of the exactly perpendicular shock, we can obtain the following equation for a compressive shock:

$$\frac{2 - \gamma}{M_a^2} r^2 + \left( \frac{\gamma}{M_a^2} + \frac{2}{M_c^2} + \gamma - 1 \right) r - (\gamma + 1) = 0, \quad (11)$$

where  $r = B_d/B_u$  is the compression ratio,  $M_a$  is the Alfvénic Mach number, which is the ratio of the upstream flow speed to the upstream Alfvén speed, and  $M_c$ , the sonic Mach number, is the ratio of the upstream flow speed to the upstream sound speed. If  $\gamma < 2$ , there is just one physical solution for the compression ratio. Here, we let  $\gamma = \frac{5}{3}$ , which indicates an adiabatic process.

Equations (5)–(10) only give the relationship between the plasma parameters upstream and downstream just at the discontinuity surface. The plasma states behind the shock interface are unknown. We still use the compression ratio  $r$  to describe the enhancement of the post-shock magnetic field relative to the origin field strength. Since the shock is generally driven by some fast moving ejecta, the compression ratio should not be constant but increases after the shock, i.e., at the position closer to the shock driver gas, the compressed magnetic field is more intense compared with the original field strength. To simplify the problem, we assume the compressed region between the shock and its driver gas is wide enough, and only the region approaching to the shock interface is considered. Therefore, we

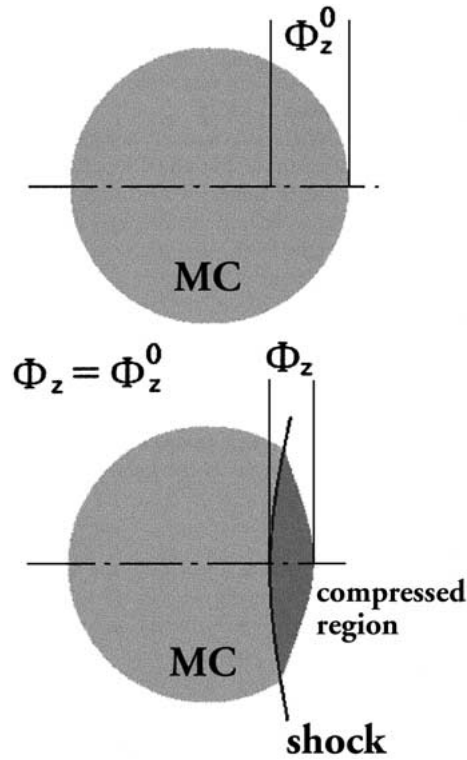


Figure 2. Sketch of the shock advancing into preceding magnetic cloud.

may ignore such a variation of the compression ratio and let it be a constant behind the shock.

### 2.3. MAGNETIC FLUX

If the magnetic field within the cloud is frozen-in, the magnetic flux is conserved. According to this assumption, we can obtain the passage time  $\Delta t$  of the compressed part of the cloud by the following equation:

$$\Phi_z = \int_0^{\Delta t} B_z v dt = \int_0^{\Delta t^0} B_z^0 v^0 dt \quad , \quad (12)$$

where  $\Phi_z$  is the magnetic flux in the  $z$  direction,  $v = v_x$  is the solar wind speed, and  $t$  is the time. The superscript '0' indicates the situation without an overtaking shock's compression. A sketch is shown in Figure 2. Obviously, the larger the compression ratio is, the more oblate is the cloud, and the shorter is the passage time  $\Delta t$ .

## 2.4. GEOMAGNETIC DISTURBANCE

Geomagnetic disturbances contributed by interplanetary  $B_s$  events can be described by the  $Dst^*$  index. The relationship between  $Dst^*$  value and interplanetary parameters has been studied by many authors (e.g., Burton, McPherron, and Russell, 1975; Akasofu, 1981; Gonzalez and Tsurutani, 1987; Gonzalez *et al.*, 1989, 1994; Prigancova and Feldstein, 1992; Vassiliadis *et al.*, 1999). A general formula is given by

$$\frac{dDst^*(t)}{dt} = Q(t) - \frac{Dst^*}{\tau}, \quad (13)$$

where  $Q$ , namely a ‘coupling function’, indicates the rate of energy input from the interplanetary medium into the ring current and  $\tau$  is the decay time.

The interplanetary southward component  $B_s$  of magnetic field, solar wind speed  $v$  and density  $\rho$  play important roles in affecting Earth’s magnetosphere. How to choose the best suitable coupling function is a key problem for predicting the level of geomagnetic disturbance. According to previous studies, the simple coupling function  $vB_z$  was widely used, and was well correlated to the observed value (Gonzalez *et al.*, 1994; Vennerstroem, 2001). Using a more complicated function does not improve the correlations significantly. Here, we also use this simple function  $vB_z$  to study the geoeffectiveness of a shock overtaking a preceding magnetic cloud.

Generally, the decay time  $\tau$  is not constant during the geomagnetic storm (Gonzalez *et al.*, 1989; Prigancova and Feldstein, 1992). The smaller the  $Dst^*$  is, the shorter is the decay time. It was suggested that the  $\tau$  is about 1 hour at the peak of the main phase of intense geomagnetic storm, and approximately 5–10 hours during the recovery phase. However, a recent statistical study (Vennerstroem, 2001) implied that the deviation of the results between the constant  $\tau$  and non-constant  $\tau$  is not obvious. Thus, we adopt  $\tau = 8$  hours in calculating the  $Dst^*$  value in this paper.

## 2.5. SUMMARY

Summarizing, we apply the following main assumptions in our theoretical analysis: (1) the magnetic cloud is described by Lundquist solution with its axis lying in ecliptic plane and perpendicular to the Sun–Earth line; (2) an exactly perpendicular shock is considered; (3) the compression ratio  $r$  is constant throughout the compressed part of the cloud; (4) the flow is ideal and the conservation of magnetic flux is therefore satisfied; and (5) the simple coupling function  $vB_z$  is adopted with constant decay time  $\tau$ . Since many assumptions are applied here, the theoretical analysis only reveals the fundamental evolution characteristics of a shock overtaking a preceding cloud. It primarily answers the question: how deeply does the shock enter the preceding MC when its geoeffectiveness reaches maximum?

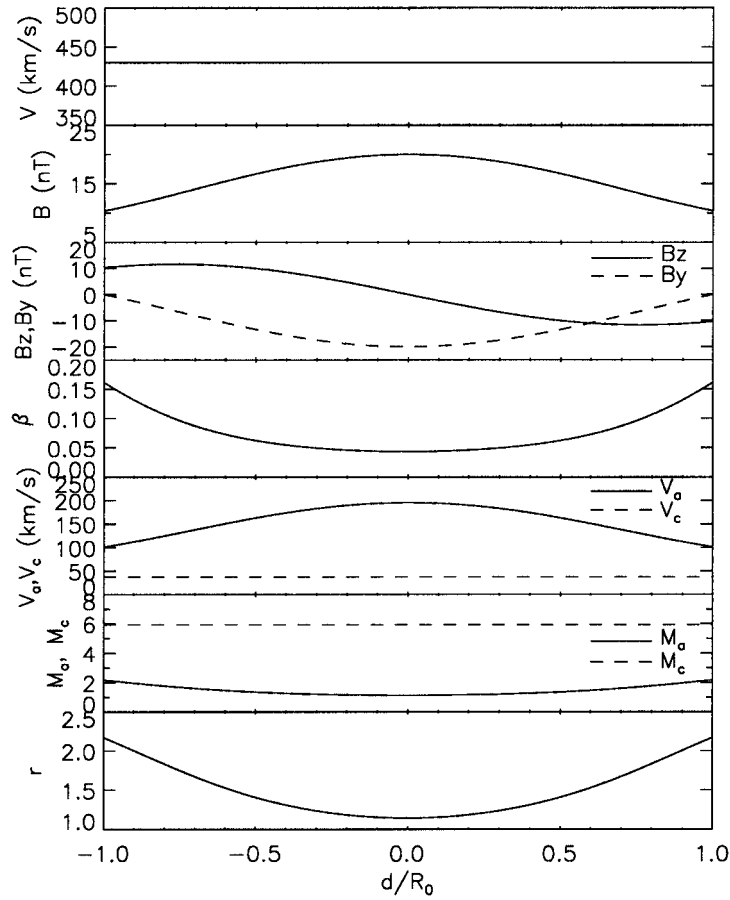


Figure 3. The variations of some parameters within the cloud. From top to bottom are plotted: solar wind speed  $v$ , magnetic field strength  $B$ ,  $z$  component field  $B_z$  (solid line) and  $y$  component  $B_y$  (dashed line) of magnetic field, the ratio of thermal pressure to magnetic pressure  $\beta$ , Alfvénic speed  $V_a$  (solid line) and sonic speed  $V_c$  (dashed line), Alfvénic Mach number  $M_a$  (solid line) and sonic Mach number  $M_c$  (dashed line), and the calculated compression ratio  $r$ .  $R_0$  is the radius of the cloud.

### 3. Results

The strength of the magnetic field at the cloud's axis is taken as  $B_0 = 20$  nT, the solar wind speed  $v = 430$  km s<sup>-1</sup>, and the density and the temperature are uniform throughout the cloud. Figure 3 shows the profiles of some parameters within the cloud. Since the strength of the magnetic field is different at different positions within the MC, the Alfvénic wave speed  $V_a$  and Alfvénic Mach number  $M_a$  vary. Approaching the center of the cloud,  $\beta$  decreases,  $V_a$  increases, and  $M_a$  and the compression ratio  $r$  therefore decrease simultaneously. In this case,  $r$  is more than 2.0 at the borders and approaches 1.0 at the center.

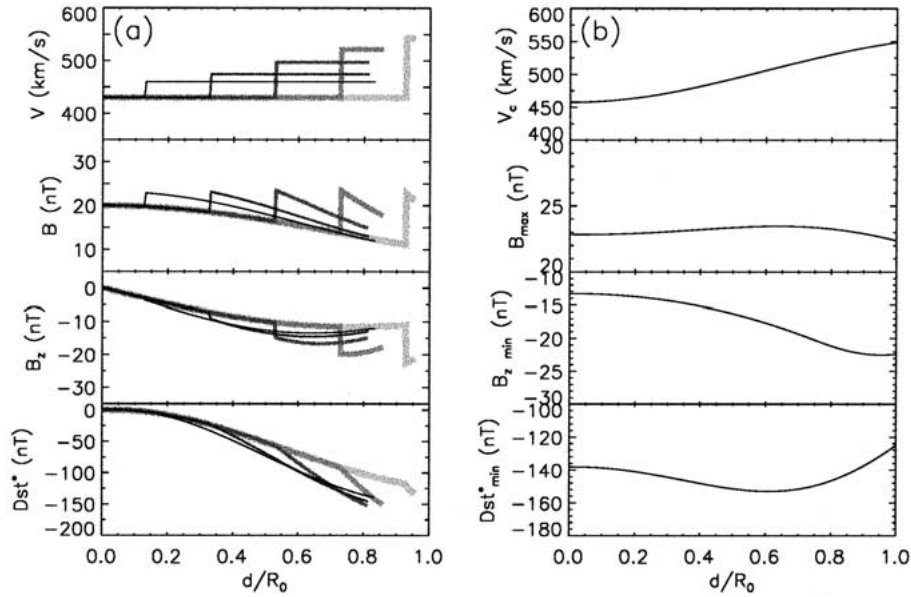


Figure 4. The evolution of a shock advancing into a preceding MC. (a) The solar wind speed  $v$ , total strength magnetic field  $B$ ,  $z$  component  $B_z$  of magnetic field, and estimated  $Dst^*$  are plotted respectively. (b) The curves of the solar wind speed  $v_c$  immediately after shock compression, the maximum  $B_{max}$  of magnetic field strength within the cloud, the minimum  $B_{z\ min}$  of the southward component of the magnetic field, and the corresponding  $Dst^*_{min}$  value versus the shock penetration depth  $d/R_0$ , respectively.

A fast forward shock overtaking the cloud with a speed of  $650\text{ km s}^{-1}$  is introduced. We only consider the last half portion of the cloud, in which the  $z$  component of magnetic field is southward. Figure 4(a) shows the evolution of such a shock advancing into such a preceding MC. The denser and thinner curves denote that the shock enters the cloud more deeply.

When the shock just enters the preceding cloud, the compression ratio is the largest, and therefore the enhancements of the magnetic field and solar wind speed are the largest. The cloud also becomes oblate simultaneously due to the conservation of magnetic flux. While the shock keeps advancing into the cloud, the maximum values of solar wind speed  $v$  decline continuously. As is well known, the large southward magnetic field  $B_s$ , i.e.,  $-B_{z\ min}$ , does not increase monotonically in this case. The corresponding minimum value of  $Dst^*$  does not monotonically decrease as shown in the last panel of Figure 4(a). There is a position where the shock compression of the preceding cloud reaches the maximum geoeffectiveness.

This characteristic is shown more clearly in Figure 4(b). Here, we use the variable  $d$ , the distance from the cloud's center, to describe the shock position relative to the cloud. As mentioned above, the solar wind speed immediately after the shock

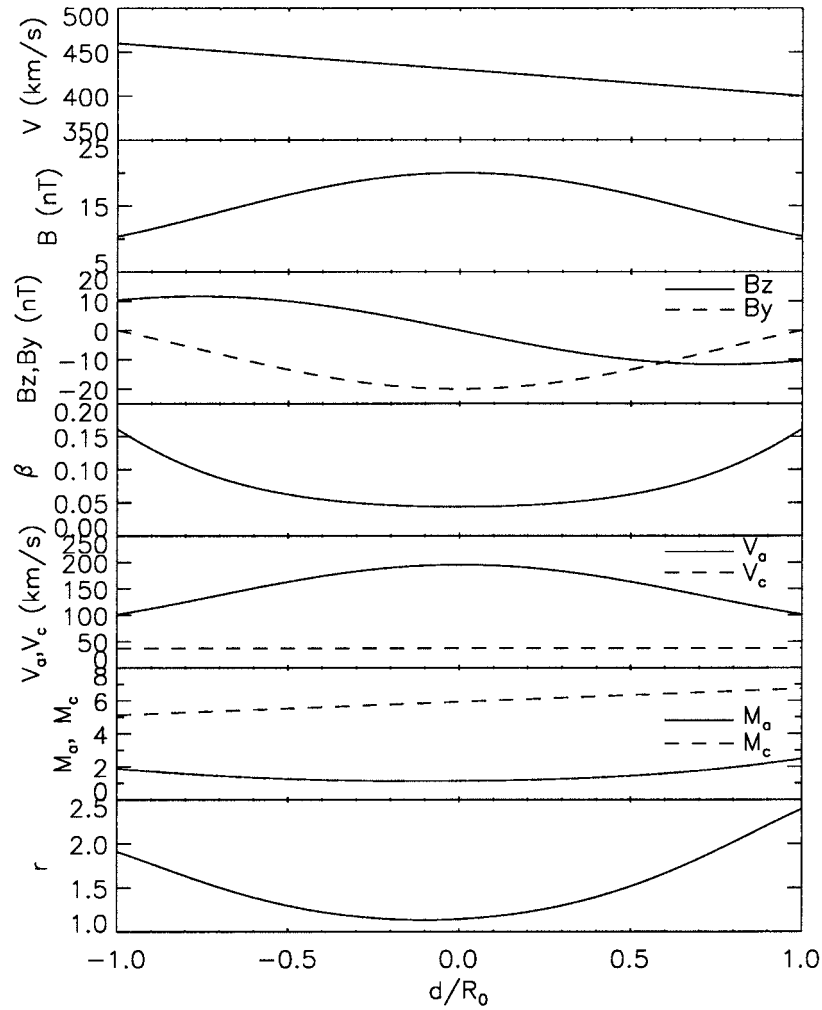


Figure 5. The variation of some parameters within an expanding cloud.

decreases monotonically while the shock penetrates the cloud. The maximum value of magnetic field strength increases first, then decreases. The minimum value of  $B_z$  has an extreme value at the position  $d = d_{B_z} = 0.95 R_0$ . Relative to the original value of  $-11.6$  nT,  $B_{z\min} = -22.5$  nT strengthens 94% due to the shock compression. The variation of the level of the corresponding estimated geomagnetic disturbance is somewhat similar to the magnetic field strength. Before the shock catches up with the cloud, i.e.,  $d \geq R_0$ , the  $Dst_{\min}^*$  caused only by the MC is  $-124$  nT. When the shock is at the cloud's center,  $d = 0$ , the estimated  $Dst_{\min}^*$  is  $-138$  nT. The largest geomagnetic storm ( $Dst_{\min}^* = -153$  nT) appears at the position where  $d = d_{Dst^*} = 0.61 R_0$ . Compared to the situation without the shock compression, the increment  $\Delta Dst_{\min}^*/Dst_{\min}^*$  of the storm intensity is about 23%.

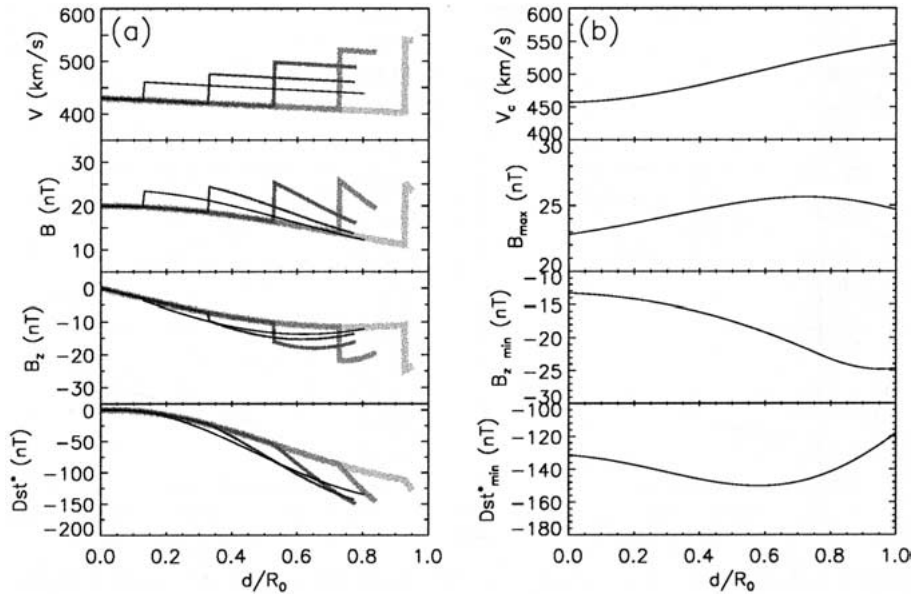


Figure 6. The evolution of a shock advancing into an expanding MC.

It should be noted that  $d_{Dst^*}$  is not equal to  $d_{B_z}$  though southward magnetic field is of great importance to the geomagnetic disturbance.

If the expansion of the magnetic cloud is considered, the solar wind speed profile should present a slope within the cloud, as shown in the first panel of Figure 5. Here, the expansion speed we use is  $30 \text{ km s}^{-1}$ , about half of the local Alfvénic wave speed, which is agreement with the observations (Klein and Burlaga, 1982). Contrary to the non-expanding case, the Alfvénic and sonic Mach numbers and the compression ratio are not symmetrical to the center of the cloud under the effect of its expansion (Figure 5).

However, the results of this case are similar to the non-expansion case. Figure 6 presents the results.  $B_{z\ min}$  reaches an extreme value at  $d = d_{B_z} = 0.95 R_0$  with decrement  $\Delta B_{z\ min}/B_{z\ min}$  of 1.14 times. The value of the estimated  $Dst^*_{min}$  also decreases first, then increases slowly. Before the shock catches up with the cloud,  $d \geq R_0$ , the  $Dst^*_{min}$  caused by the MC is  $-117 \text{ nT}$ . When the shock is at the cloud's center,  $d = 0$ , the estimated  $Dst^*_{min}$  is  $-131 \text{ nT}$ . The largest geomagnetic storm ( $Dst^*_{min} = -150 \text{ nT}$ ) appears when  $d = d_{Dst^*} = 0.59 R_0$ . The increment of the storm intensity relative to the non-compressed situation is about 28%. Compared with the previous case, the position of the shock associated with the largest storm is slightly deeper and the increment  $\Delta Dst^*_{min}/Dst^*_{min}$  becomes larger.

The above cases are all associated with a shock speed of  $650 \text{ km s}^{-1}$ . The results suggest that the geoeffectiveness of such an event does not always increase while the shock advances into the preceding MC. To find the dependence of such depth, we further investigate many cases with various shock speeds. Obviously,

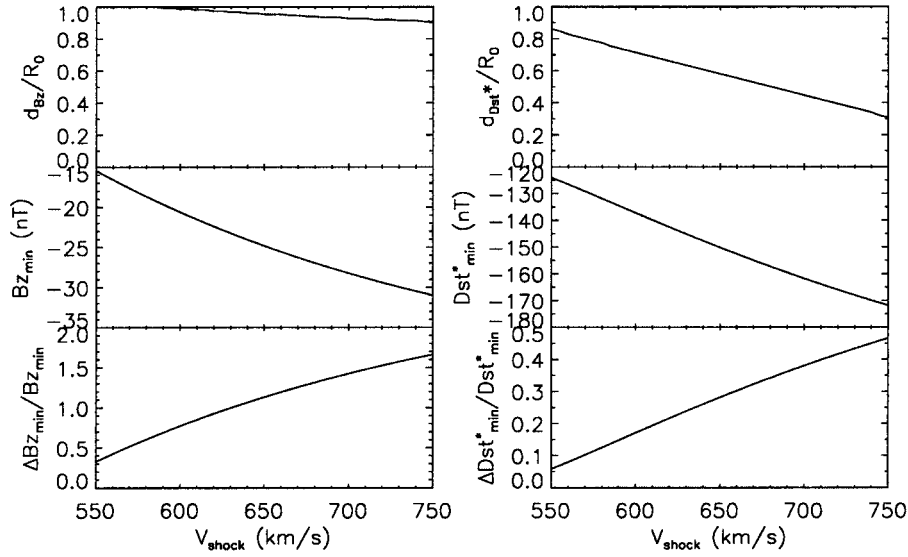


Figure 7. Left column: the distance  $d_{B_z}$  from the cloud's center, the value of  $B_{z \text{ min}}$ , and its percentage of increment versus the shock speed  $V_{\text{shock}}$ , respectively. Right column: the distance  $d_{Dst^*}$  from the cloud's center, the value of  $Dst^*_{\text{min}}$ , and its percentage of increment versus the shock speed  $V_{\text{shock}}$ , respectively.

$B_{z \text{ min}}$ ,  $\Delta B_{z \text{ min}}/B_{z \text{ min}}$ ,  $Dst^*_{\text{min}}$ ,  $\Delta Dst^*_{\text{min}}/Dst^*_{\text{min}}$ , and their corresponding position  $d_{B_z}$  and  $d_{Dst^*}$  should also change. Figure 7 shows these variables versus the shock speed  $V_{\text{shock}}$ . As presented in the left column,  $d_{B_z}$  is larger than  $0.9 R_0$ . As the shock speed increases,  $d_{B_z}$  declines slightly. The value of  $B_{z \text{ min}}$  decreases from  $-15.4$  nT to  $-31.0$  nT due to the intensifying of the shock. Simultaneously, the value of  $\Delta B_{z \text{ min}}/B_{z \text{ min}}$  increases from 0.33 to 1.66 monotonically. The behavior of  $Dst^*_{\text{min}}$  is similar to  $B_{z \text{ min}}$  except for the position  $d_{Dst^*}$ . The change of  $d_{Dst^*}$  is obvious. The more intense the overtaking shock is, the smaller is the value of  $d_{Dst^*}$ , which indicates that the shock enters the preceding magnetic cloud more deeply.  $Dst^*_{\text{min}}$  also descends monotonically with the increase of the shock speed, and  $\Delta Dst^*_{\text{min}}/Dst^*_{\text{min}}$  rises correspondingly. When  $V_{\text{shock}} = 550 \text{ km s}^{-1}$ ,  $d_{Dst^*} = 0.86 R_0$ ,  $Dst^*_{\text{min}} = -124$  nT, and  $\Delta Dst^*_{\text{min}}/Dst^*_{\text{min}} = 6\%$ . When  $V_{\text{shock}}$  increases to  $750 \text{ km s}^{-1}$ ,  $d_{Dst^*} = 0.31 R_0$ ,  $Dst^*_{\text{min}} = -172$  nT, and  $\Delta Dst^*_{\text{min}}/Dst^*_{\text{min}} = 47\%$ .

Generally, a shock should be decaying due to the interaction with the ambient solar wind while propagating in the interplanetary medium. Hence, the value of  $d_{Dst^*}$  should be larger than the above estimates in reality.

#### 4. Discussion and Summary

In our modeling,  $Dst^*$  is used as the index of the geomagnetic disturbance. It should be noted that  $Dst^*$  is different from the measured  $Dst$  index.  $Dst^*$  is the

$Dst$  value after a correction due to magneto-pause currents is made. The relationship between  $Dst^*$  and  $Dst$  is usually given (e.g., Burton, McPherron, and Russell, 1975) by

$$Dst^* = Dst - bp^{1/2} + c, \quad (14)$$

where  $p$  is the solar wind dynamic pressure during the storm,  $b$  is a proportionality factor, and  $c$  is the quiet time solar wind dynamic pressure contribution. Generally, the  $Dst^*$  value is close to the  $Dst$  value. However, in some events associated with large solar wind dynamic pressure variations,  $Dst^*$  may be much smaller than measured  $Dst$  (Tsurutani *et al.*, 1992b). During such intervals, extraordinary pressure may push the magneto-pause closer to the Earth, and therefore cause outage of telecommunications cable lines perhaps (Anderson, Lanzerotti, and MacLennan, 1974; Lanzerotti, 1992). Thus, some dramatic occurrences are usually not related to the largest  $Dst$  events but to the largest  $Dst^*$  events. Maybe using  $Dst^*$  is more valuable for prediction of space weather.

Although the southward magnetic field  $B_s$  is very important in producing geomagnetic storms, the results suggest that the position where  $B_{z\min}$  reaches the minimum value is not the same as the position where  $Dst_{\min}^*$  reaches the minimum value. This conclusion is reasonable because the geomagnetic storm is not only related to  $B_s$ , but also related to solar wind speed, the duration  $\Delta t$  of  $B_s$ , and so on. While  $B_s$  increases due to shock compression,  $\Delta t$  will be shortened simultaneously.

In this paper, an exactly perpendicular shock is assumed. Actually, the normal direction of overtaking shocks is not perpendicular to the magnetic fields though many shocks roughly propagate toward the Earth, and the direction of the magnetic field should rotate by some angle across the shock interface. As for a fast shock, the magnetic field will bend away from the normal, which usually increases the magnitude of the preexisting  $z$  component of the magnetic field. Hence, in the case of an oblique shock, the elevation angle change of the magnetic field is usually favorable to its geoeffectiveness as presented in the October 2001 event (Figure 8). The advancing shock not only compressed the preexisting magnetic field, but also rotates the field vector more southward as shown in the second panel of Figure 8. The details of this event and other similar events will be presented in another paper.

If shock moves enough faster than the preceding magnetic cloud or the initial time interval between them is very short, the shock can overtake and exceed the cloud probably before their arrival at 1 AU. Our theory is too simple to be suitable for such case. Shocks are commonly driven by interplanetary ejecta. After a shock passes the preceding cloud, its driver gas will overtake the cloud, interact with it, and therefore form a complex interplanetary structure (Burlaga *et al.*, 2001; Burlaga, Plunkett, and St. Cyr, 2002). Multiple magnetic cloud (Wang, Wang, and Ye, 2002) is one kind of complex structure, which also may create a great geomagnetic storm probably due to the compression between the sub-clouds, such as 31 March 2001 event (Wang, Ye, and Wang, 2003a, b).

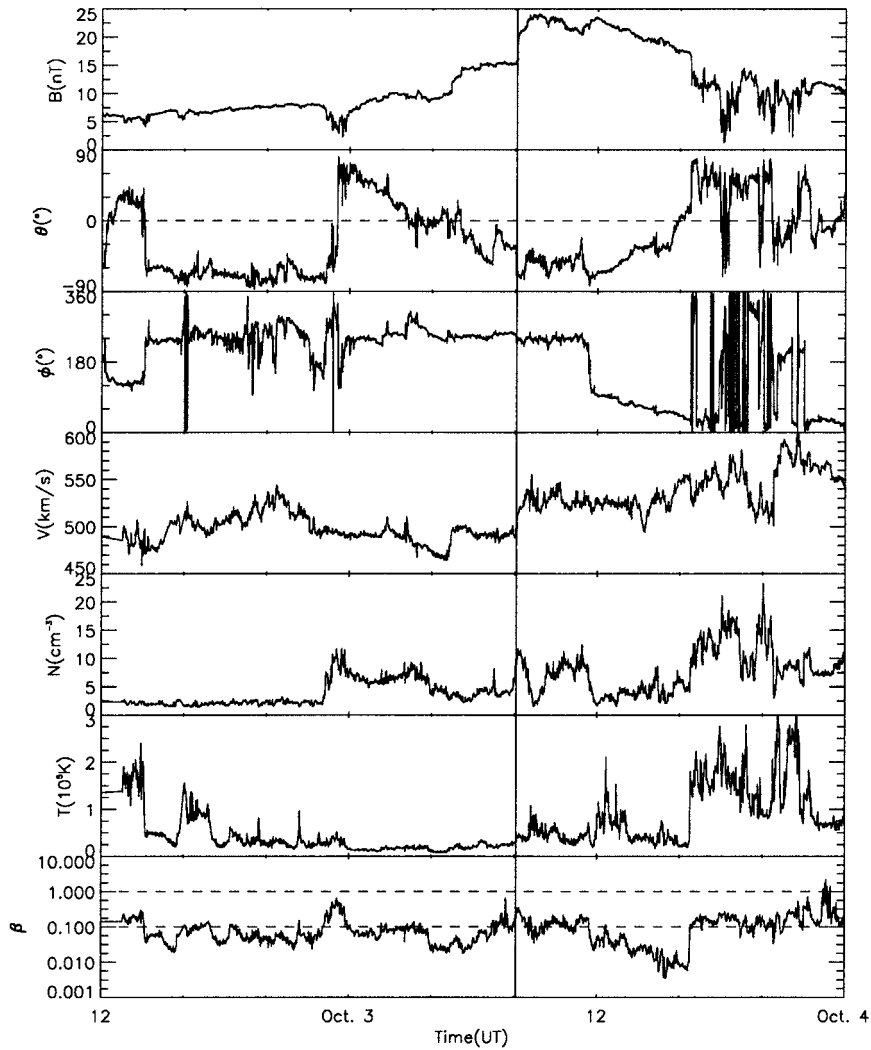


Figure 8. Observations by the ACE spacecraft from 12:00 UT 2 October through 3 October 2001 (in GSM). From *top to bottom* are plotted: magnetic field strength  $B$ , the elevation  $\theta$  and azimuthal  $\phi$  angles of the field direction, bulk flow speed  $V$ , proton density  $N$ , the proton temperature  $T$ , and the ratio of thermal pressure to magnetic pressure  $\beta$ .

Figure 9 shows an event of fast forward shocks penetrating a preceding magnetic cloud, which has been reported recently by Wang *et al.* (2003). S1 labeled in this figure indicates a magneto-sonic wave, which likely decayed from a shock due to the decrease of the local  $\beta$  and the dissipation of S1 while advancing into the cloud. S2 is a fast forward shock with the speed of approximately  $550 \text{ km s}^{-1}$ . According to our theory, the corresponding  $d_{D_{S1}^*}$  should be about  $0.86 R_0$ . Obviously, the shock just entered the cloud at 1 AU in this event. Thus, we suspect that

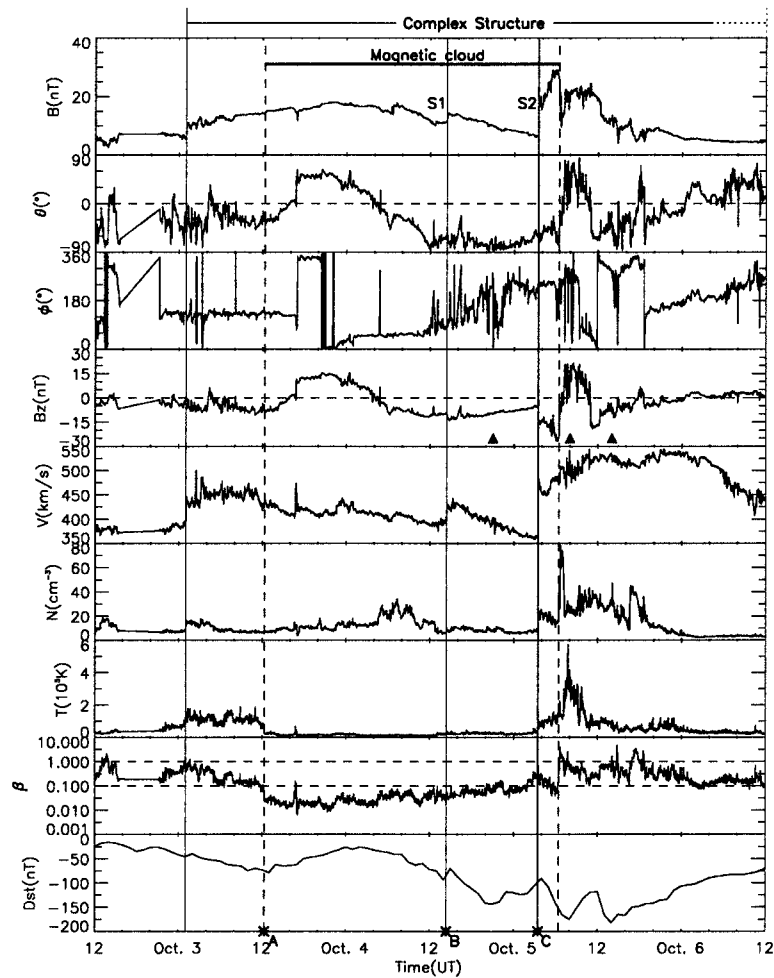


Figure 9. Observations by the WIND spacecraft from 12:00 UT 2 October to 12:00 UT 6 October 2000 (in GSM). From top to bottom are plotted: magnetic field strength  $B$ , the elevation  $\theta$  and azimuthal  $\phi$  angles of the field direction,  $z$  component field  $B_z$ , bulk flow speed  $V$ , proton density  $N$ , the proton temperature  $T$ , the ratio of thermal pressure to magnetic pressure  $\beta$ , and the geomagnetic index  $Dst$ . (From Wang *et al.*, 2003).

this event has almost reached the maximum geoeffectiveness. Three peaks of  $Dst$  are denoted in the fourth panel by filled triangles. The first  $Dst$  peak ( $= -143$  nT) was caused by  $B_s$  intrinsic to the magnetic cloud, the second peak ( $= -175$  nT) was produced by the shock compression of the preceding cloud, and the last peak ( $= -182$  nT) was created by  $B_s$  intrinsic to the shock driver gas. By comparing the first two peaks, we find that the increment of the storm intensity is about 22%, but not consistent with the estimated value 6%. This inconsistency maybe is due to the too simple theoretical model and the difference between  $Dst$  and  $Dst^*$ . The actual intensity of the geomagnetic storm is larger than the theoretical estimation.

We evaluate the geoeffectiveness of a shock overtaking a preceding magnetic cloud by using a simple theoretical model. The obtained results are substantial and meaningful though lots of assumptions are applied in this model. On the basis of the theoretical analysis, it is possible to improve the prediction of the extraordinary geomagnetic storms due to the compression of shock.

### Acknowledgements

We acknowledge the use of the data from ACE and WIND spacecraft and the *Dst* index from World Data Center. This work is supported by the National Natural Science Foundation of China (49834030), the State Ministry of Science and Technology of China (G2000078405), and the Chinese Academy of Sciences (KZCX2-SW-136).

### References

- Akasofu, S.-I.: 1981, *Space Sci. Rev.* **28**, 121.
- Anderson, C. W. III, Lanzerotti, L. J., and MacLennan, C. G.: 1974, *The Bell System Tech. J.* **53**, 1817.
- Burlaga, L. F.: 1988, *J. Geophys. Res.* **93**, 7217.
- Burlaga, L. F., Behannon, K. W., and Klein, L. W.: 1987, *J. Geophys. Res.* **92**, 5725.
- Burlaga, L. F., Plunkett, S. P., and St. Cyr, O. C.: 2002, *J. Geophys. Res.* **107**, 1266.
- Burlaga, L., Sittler, E., Mariani, F., and Schwenn, R.: 1981, *J. Geophys. Res.* **86**, 6673.
- Burlaga, L. F., Skoug, R. M., Smith, C. W., Webb, D. F., Zurbuchen, T. H., and Reinard, A.: 2001, *J. Geophys. Res.* **106**, 20957.
- Burton, R. K., McPherron, R. L., and Russell, C. T.: 1975, *J. Geophys. Res.* **80**, 4204.
- Cane, H. V., Richardson, I. G., and Wibberenz, G.: 1997, *J. Geophys. Res.* **102**, 7075.
- Erkaev, N. V., Farrugia, C. J., Biernat, H. K., Burlaga, L. F., and Bachmaier, G. A.: 1995, *J. Geophys. Res.* **100**, 19919.
- Gonzalez, W. D. and Tsurutani, B. T.: 1987, *Planetary Space Sci.* **35**, 1101.
- Gonzalez, W. D., Tsurutani, B. T., and Gonzalez, A. L. C.: 1999, *Space Sci. Rev.* **88**, 529.
- Gonzalez, W. D., Tsurutani, B. T., Gonzalez, A. C., Smith, E. J., Tang, F., and Akasofu, S.-I.: 1989, *J. Geophys. Res.* **94**, 8835.
- Gonzalez, W. D., Joselyn, J. A., Kamide, Y., Kroehl, H. W., Rostoker, G., Tsurutani, B. T., and Vasylunas, V. M.: 1994, *J. Geophys. Res.* **99**, 5771.
- Gosling, J. T., McComas, D. J., Phillips, J. L., and Bame, S. J.: 1991, *J. Geophys. Res.* **96**, 731.
- Gosling, J. T., McComas, S. J., Phillips, J. L., and Bame, S. J.: 1992, *J. Geophys. Res.* **97**, 6531.
- Klein, L. W. and Burlaga, L. F.: 1982, *J. Geophys. Res.* **87**, 613.
- Kumar, A. and Rust, D. M.: 1996, *J. Geophys. Res.* **101**, 15667.
- Lanzerotti, L. J.: 1992, *Geophys. Res. Lett.* **19**, 1991.
- Lepping, R. P., Burlaga, L. F., Szabo, A., Ogilvie, K. W., Mish, W. H., Vassiliadis, D., Lazarus, A. J., Steinberg, J. T., Farrugia, C. J., Janoo, L., and Mariani, F.: 1997, *J. Geophys. Res.* **102**, 14049.
- Lundquist, S.: 1950, *Arkiv Fys.* **2**, 361.
- Prigancova, A. and Feldstein, Ya. I.: 1992, *Planetary Space Sci.* **40**, 581.
- Sheeley, N. R., Howard, R. A., Koomen, M. J., Michels, D. J., Schwenn, R., Muhlhauser, K.-H., and Rosenbauer, H.: 1985, *J. Geophys. Res.* **90**, 163.

- Tsurutani, B. T., Gonzalez, W. D., Tang, F., Akasofu, S. I., and Smith, E. J.: 1988, *J. Geophys. Res.* **93**, 8519.
- Tsurutani, B. T., Gonzalez, W. D., Tang, F., and Lee, Y. T.: 1992a, *Geophys. Res. Lett.* **19**, 73.
- Tsurutani, B. T., Gonzalez, W. D., Tang, F., Lee, Y. T., and Okada, M.: 1992b, *Geophys. Res. Lett.* **19**, 1993.
- Vassiliadis, D., Klimas, A. J., Valdivia, J. A., and Baker, D. N.: 1999, *J. Geophys. Res.* **104**, 24957.
- Vennerstroem, S.: 2001, *J. Geophys. Res.* **106**, 29175.
- Wang, Y. M., Wang, S., and Ye, P. Z.: 2002, *Solar Phys.* **211**, 333.
- Wang, Y. M., Ye, P. Z., and Wang, S.: 2003a, *Chinese J. Geophys.*, submitted.
- Wang, Y. M., Ye, P. Z., and Wang, S.: 2003b, *J. Geophys. Res.*, submitted.
- Wang, Y. M., Ye, P. Z., Wang, S., and Xue, X. H.: 2003, *Geophys. Res. Lett.*, in press.
- Webb, D. F. and Howard, R. A.: 1994, *J. Geophys. Res.* **99**, 4201.
- Wilson, R. M. and Hildner, E.: 1984, *Solar Phys.* **91**, 168.
- Zhang, G. and Burlaga, L. F.: 1988, *J. Geophys. Res.* **93**, 2511.